

2016

Parameterisation of intra array effects around Wind Turbine Monopiles

Needham, M.

Needham, M. (2016) 'Parameterisation of intra array effects around Wind Turbine Monopiles', The Plymouth Student Scientist, 9(2), p. 160-194.

<http://hdl.handle.net/10026.1/14132>

The Plymouth Student Scientist
University of Plymouth

All content in PEARL is protected by copyright law. Author manuscripts are made available in accordance with publisher policies. Please cite only the published version using the details provided on the item record or document. In the absence of an open licence (e.g. Creative Commons), permissions for further reuse of content should be sought from the publisher or author.

Parameterisation of intra array effects around Wind Turbine Monopiles

Part II: Analysis and conclusions drawn from laboratory testing of TKE and bed shear around Monopiles subjected to current and varying angles of wave propagation.

Maxwell Needham

Project Advisor: [Dave Simmonds](#), School of Marine Science and Engineering, Plymouth University, Drake Circus, Plymouth, PL4 8AA

Abstract

Project II is a continuation of project I which studied the effects of wave incidence angle and current interaction around offshore Wind Turbine Monopiles. This report presents a brief recap of project I findings and objectives before identifying the experimental methodology used for lab testing, post processing and results analysis. Laboratory testing conducted in the Plymouth Coast basin used a 1:50 scale Monopile to replicate the prototype site and conditions of Scroby Sands Offshore Windfarm. Turbulent Kinetic Energy (TKE) and Bed Shear Stress were measured across the wake region as part of this testing, enabling a number of conclusions to be drawn. Firstly, it was noted when wave and current propagation directions were more aligned a higher level of TKE is noted at both bed and free stream level, this was seen to decay to background levels along the downstream centreline from the Monopile at around 14 diameters at free stream level. At bed level it took 8 Monopile diameters downstream to decay which was different to that predicted in Rogan's (2015) work. Secondly, the turbulent wake region was seen to have rotated anticlockwise under wave conditions to align more with incident wave direction; this was particularly seen when wave propagation angles aligned with those of the current. Thirdly, Bed Shear Stress was observed along the downstream centreline from the Monopile. Although no clear relationships were observed, it was noted that a slightly higher level of Bed Shear Stress was seen when waves and currents were propagated at perpendicular angles. This testing also confirmed that the observed Bed Shear Stress, when scaled, matched in magnitude that of Scroby Sands prototype site. The need for research in this specific area of current and wave interaction around Monopiles is of high importance in order to bring down development costs of offshore renewables therefore a number of recommendations for further research have been made in this report.

Contents

1.0 Introduction	163
2.0 Objectives of Project I & Project II	163
3.0 Coastal basin set up and lab work methodology	164
3.1 Coastal laboratory basin layout and equipment.....	164
3.2 Wave and current basin setup	166
4.0 ADV Raw data processing methodology	167
4.1 Data processing.....	167
4.2 Matlab data processing overview.....	168
4.3 Denoising	168
4.3.1 Removing wave effects from velocity traces	169
4.3.2 Bed shear extraction	170
5.0 Results of lab experimentation	171
5.1. Discussion of data	171
5.2. Data Limitations	172
5.2.1 Data accuracy limitations.....	172
5.2.2 Scaling issues.....	173
5.2.3 ADV wave component removal via matlab	173
5.3. Observations	173
5.3.1 Analysis of wave propagation angles on TKE distribution	173
5.3.2 Analysis of TKE decay downstream of the Pile	176
5.3.3 Analysis of bed shear stress downstream of the Pile	179
5.4. Summary of Results	181
6.0 Discussion of findings.....	182
6.1 TKE distribution in Wake Region.....	182
6.2 Wake Region TKE decay	183
6.3 Downstream bed shear stress	185
7.0 Conclusions	189
7.1. Links to previous research	190
7.2. Real world application	191
7.3 Further proposed research	191
References	193

Table of Figures

Figure 1 - Coastal Basin set up prior to filling of Basin	164
Figure 2 - Seeding material being added to the Basin	165
Figure 3 - Sensor Positions achieved by traverse	166
Figure 4 – Breakdown of the Current Velocity trace into Mean Flow & Fluctuations.....	167
Figure 5 - Example denoised current only ADV X velocity traces (Blue - Original, Red - Denoised)...	168
Figure 6- Example ADV Energy density plot from Vector2turb1 Matlab script Jon Miles (2003) – Data taken from Position 7 with +20 degree waves	169
Figure 7 - X, Y & Z Ln Spectral Energy density plots showing removed wave frequency bands – Data taken from Position 7 with +20 degree waves	170
Figure 8 - Calculating Bed Shear $m (du/dz)$ values	171
Figure 9 – Superimposed Wave tests (Amplitude accuracy check) – 1cm (0.01cm) Specified wave amplitude	172
Figure 10 - TKE decay in bed position along a transect 20 degrees right of the downstream centreline behind the pile	174
Figure 11 - TKE decay in bed position along a transect 20 degrees left of the downstream centreline behind the pile	175
Figure 12 - Vortex patterns from Monopiles in currents (Sumer & Fredsøe, 1997).....	176
Figure 13 - Decay of TKE from Monopile in Bed & Free stream Positions downstream of Monopile CL	176
Figure 14- Bed Position TKE along a transect downstream behind Monopile CL.....	177
Figure 15 - Free Stream Position TKE along downstream transect behind Monopile CL	178
Figure 16 - Diagram of layers within a flow (University of Illinois, No date)	179
Figure 17 - Observed Bed Shear Downstream of Monopile CL	179
Figure 18 - Rotation of wake region under negatively angled propagated waves (originating at top of diagram)	182
Figure 19 - Turbid wakes from Thanet OWF as viewed from Landsat 8 (Vanhellemont and Ruddick, 2014)	183
Figure 20 - Fluid turbulence shown using dye tracer (Tumbler, No date)	186
Figure 21 - Scroby Sands Monopile bathometric scan of wake region showing scour pit (CEFAS, 2006)	187
Figure 22 - Total Bed Shear Stress exceedance in Summer and Winter for various particle sizes.....	188

Table of Equations

Equation 1 - Turbulent Kinetic Energy Equation	167
Equation 2 - Calculating Bed Shear Stress in log layer (Crone, No date)	171
Equation 3 - Determine %EI from TKE data	173
Equation 4 - Reynolds number calculation from a Monopile in a current (Dight, 2013)	175
Equation 5 - Inferring Bed Shear Stress from TKE equation (University of Illinois, No date)	185
Equation 6 - Stoke particle settling equation (Shearer, No date)	188

1.0 Introduction

Project II is a continuation of Project I drawing on the literature and theory reviewed in the previous project with a sight to conduct extensive laboratory work. This lab work was undertaken to explore predictions made in Project I in regards to monopile turbulence wakes under varying wave angles of propagation.

Project I concluded the introduction of monopiles into offshore current and wave environments caused an array of hydrodynamic and sediment impacts which were explored through background research and theory. The literature review concluded that there was a large gap in the present understanding of wave and current interaction around monopiles outside of a flume context, specifically Rogan *et al.*, (2015) focusing on the effect of incident wave angle on the size of the downstream wake region.

This area of research holds promise as there are large post construction hydrodynamic and sediment monitoring costs associated with the construction of Offshore Wind Farms (OWFs). Presently OWFs are constructed not knowing what the likely sediment and hydrodynamic effects will be so a lot of money is spent assessing them. Knowing what to expect around turbine monopiles in tidal waters prior to construction may save a large amount of monitoring costs and post construction scour rectification bringing down associated capital costs of offshore renewables.

2.0 Objectives of Project I & Project II

The aim of project II is to use physical laboratory modelling as supposed to numerical modelling due to the higher accuracy and the availability of the COAST Basin in Plymouth University. Tests will help further clarify the relationship outlined in the below Project I question being investigated:

To what degree does the angle of wave interaction affect the turbulence downstream from the Monopile when currents exist at an intra-array scale?

This question naturally leads on to a refined hypothesis that will be investigated in Project II through lab testing and comprehensive results analysis:

TKE (Turbulent Kinetic Energy) decay at distance from the Monopile is affected by the incident angle of wave propagation when a “tidal” current is present.

In order to successfully investigate this hypothesis there were a number of primary objectives that needed to be identified in order to collect relevant laboratory data;

- 1.0 The coastal basin needed to be set up in accordance with plans set out in Part I and calibrated before data was collected.
- 2.0 Background TKE at bed and free stream height was collected at various positions behind the Monopile under a pure current condition in order to determine background TKE levels prior to combined wave and current action.

3.0 Waves were propagated at various angles at the Monopile and TKE in the wake region was observed again. Additional Bed Shear Tests were conducted in the labs for comparison to the prototype site of Scroby Sands.

From the collected data a relationship was be established between TKE (Turbulent Kinetic Energy) and the angle of wave propagations and its consequent decay at distance from the Monopile with results being critiqued in order to assure accuracy and the implication of findings will be further discussed in this report.

This investigation builds on the work of Rogan (2015), however due to the availability of a 1m x 1m traverse the collection of a vast amount of data was possible compared to Rogan's hand analysis thus giving a more detailed picture of the wake region turbulence. Project II provides a foundation for further work to be undertaken on this subject as well as giving a wider understanding of Monopile Wave and Current interaction.

3.0 Coastal basin set up and lab work methodology

3.1 Coastal laboratory basin layout and equipment

The coastal basin in Plymouth University was used for the laboratory testing over the period of the 7th to the 14th of October 2015. A health and safety risk assessment was undertaken prior to commencement of lab work to highlight and manage potential hazards, which can be found in Appendix 6.0. The basin itself is 15m long by 10m wide and was filled to a depth of 0.5m with fresh water for the duration of the testing. The Monopile being assessed in the experiment was a 10cm diameter pipe section bolted in to the bed of the basin with a flush base. A 10cm diameter pile was chosen as it gave a manageable scale factor of 50 which was comparable with wave and current scaling for the lab as well as being the same diameter as used by Rogan so results would be easily comparable. The Monopile was placed 4.7m from the wave paddles and initially at 4.5m and subsequently at 5.0m from the upstream flow straightener. A diagram showing the position of the lab layout and equipment can be found in Appendix 2.0.



Figure 1 - Coastal Basin set up prior to filling of Basin

Equipment used in the lab included two Nortek ADV (Acoustic Doppler Velocimeter) sensors (also referred to as Vectrino Profilers) used to analyse turbulence and bed shear profiles. Each sensor had a blanking distance (blind distance) from its face to where it was able to take readings so that it does not record the turbulence it created. Sensors were able to record measurements over a 3.5cm profile split into 0.1cm bin spacing's with a maximum accuracy being achieved in the 5cm bin. Sampling was taken at a rate of 64 Hz over a period of 1 minute in order to get a good size data sample.

Vectrinos were mounted at various heights within the water, the upstream sensor being mounted at 38cm above the bed in order to record the mean flow and not cause any disturbance in the current downstream. The second sensor was alternated between two depths: 45cm referred to as Free Stream height and 12cm referred to as Bed height. Seeding of the tank was necessary in order to get a satisfactory level of acoustic backscatter. Polyamide particles were liberally mixed into the tank in order to reflect the ADV signals and consequently give particle velocities via the Doppler Effect. Seeding of the tank was done regularly in order to improve data collection quality with the aim of achieving a signal to noise ratio of approximately 20-30% and a signal correlation above 70%.



Figure 2 - Seeding material being added to the Basin

A wave gauge was also installed adjacent to the upstream ADV sensor in order to assess the accuracy of the size of the waves being produced by the wave paddles, this was mounted 2.5m from the paddles and 3.75m from the flow straighteners at the upstream end of the tank so as not to interfere with any of the other equipment.

A 1m x 1m Traverse was mounted centrally behind the Monopile, this allowed the downstream ADV sensor to be moved to multiple positions quickly and with a high degree of accuracy. The traverse allowed measurements to be taken across the wake region however it restricted the width of the radii assessed (see Appendix 3 for traverse set up diagram) to 20° either side of the centreline of the Monopile downstream.

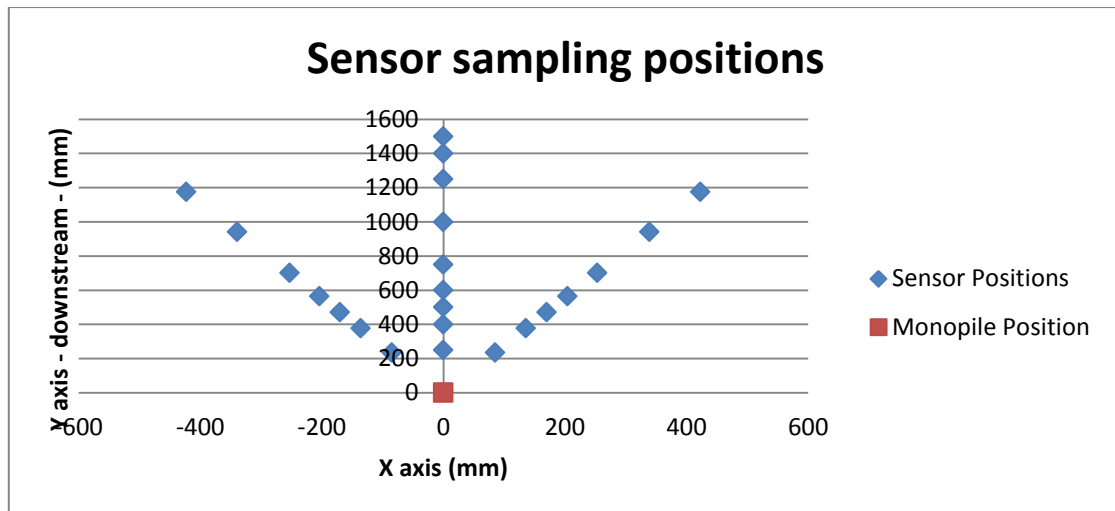


Figure 3 - Sensor positions achieved by traverse

3.2 Wave and current basin setup

The below wave and current parameters in Table 1 are taken at prototype scale as representative for Scroby Sands OWF (Offshore Wind Farm) located in the Thames estuary and have been scaled down with a scale factor of 1:50 to give the model measurement.

Table 1 - Prototype and Model parameters (Dight, 2013)

Prototype Measurement	Acronym	Reading	Unit	Model Measurement	Achieved in lab
Wave Height	Hs	0.8	m	0.016	0.02
Wave Length	L	68.82	m	1.38	1.0
Averaged Wave Period	T _{Av}	6.64	Sec	0.94	0.95
Current Velocity	V	1.26	ms ⁻¹	0.178	0.176±1 (Approx.)

It was not always possible to achieve these parameters exactly at model scale due to limitations in the wave paddles to achieve such specific wavelengths and periods however consequent implications of rough scaling will be discussed later on.

Another parameter assessed when setting up the basin was the possible angles of wave propagation, angles up to $\pm 30^\circ$ were considered. It was found that anything over $\pm 20^\circ$ caused wave reflection off the walls of the tank causing disturbance to the incident waves in the wake region therefore causing interference which would affect any readings taken in the region. The angles of wave propagation decided upon were -20° , 0° and $+20^\circ$ as shown in Appendix 2.0.

Lastly pump settings were determined in order to gain the correct model flow rate, it was found that a pump speed of -36% (minus to achieve the correct current direction) was needed to achieve a flow rate of 17.6cm/s this is close to the calculated 17.8cm/s. It must be noted since the flow speed was being measured by ADV sensors it is more sensitive to turbulence and small fluctuations in the flow over

a more traditional flow gauge so this is reflected in the fact the sensor gave a range of $\pm 1\text{cm/s}$.

4.0 ADV Raw data processing methodology

Raw ADV data requires in depth post processing in order to achieve representative and accurate results as both the data quality and the noise levels had to be assessed. Each ADV reading consists of 4 data streams corresponding to particle velocities in three vectors u , v & w (with the w vector consisting of an average of two receiver velocities), each of which must be assessed individually before being combined to give a TKE reading as shown in Equation 1 below.

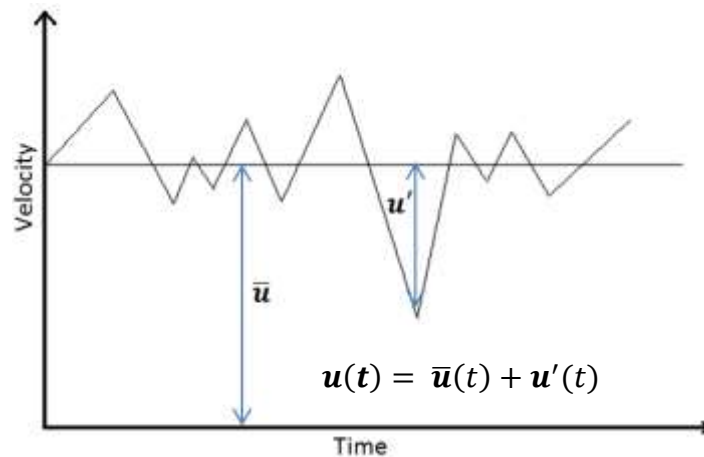


Figure 4 – Breakdown of the Current Velocity trace into Mean Flow & Fluctuations

$$\text{TKE} = \frac{1}{2} \rho \left(\overline{u'^2} + \overline{v'^2} + \overline{w'^2} \right) \quad [1]$$

Equation 1 - Turbulent Kinetic Energy Equation

4.1 Data processing

An awareness of noise within in the data is important as the sensors work by bouncing signals off seeding particles and using the Doppler Effect to determine their velocity from the returning signal. Occasionally the received speeds can be recorded incorrectly as the levels of seeding are too low in that moment so the returning/reflected signals can be confused and result in false large velocity spikes in data records. If these spikes then are recorded as part of the data, when velocities are averaged this can undermine the accuracy of the data, consequently de-noising needed to be considered. Rogan used a modified version of Goring and Nikora (2002) where by velocities were plotted against their first and second derivatives in 3D space with points falling outside a defined volume being excluded. This method is considered more applicable than a simple signal to noise (S/N) ratio threshold (Rogan *et al.*, 2015).

It was decided that filtering data using purely correlation and signal to noise thresholds was impractical due to substantial fluctuations within datasets of these two variables which would consequently result in the blanket discarding of data

points. Since the seeding of the basin was kept in check throughout the experiments it is reasonable to purely interrogate recorded the data

4.2 Matlab data processing overview

Two varieties of TKE data were collected that in turn needed analysing differently; firstly ADV data collected under current only conditions only and secondly ADV data collected under current and wave conditions. ADV data collected under purely current conditions only needed denoising so was relatively easy to process. ADV data collected under wave and current conditions was much harder to process due to the velocity trace being affected by the wave motion. This process is broken down further and explained in the *Removing wave effects from velocity traces* section 4.3.2 below.

4.3 Denoising

A simple way of detecting noise and data errors was excluding data ± 3 standard deviations from the mean as this is statistically where 99.8% of the data should lie thereby excluding the spikes. This works on the assumption that the turbulence velocities fit a normal distribution around the mean velocity, this is a fair assumption as turbulence by its very nature is random so should conform. A nine point moving average filter was then used to smooth the data to remove any further peaks missed by the first filter. This was done to discard any readings that are vastly larger or smaller than the moving average which is characteristic of noise spikes smaller than three times the standard deviation that would not be picked out by the first filter. Both of these filters, supplied by J. Miles (2003), were applied to the data in matlab rather than excel as this was the most efficient programme for data processing.

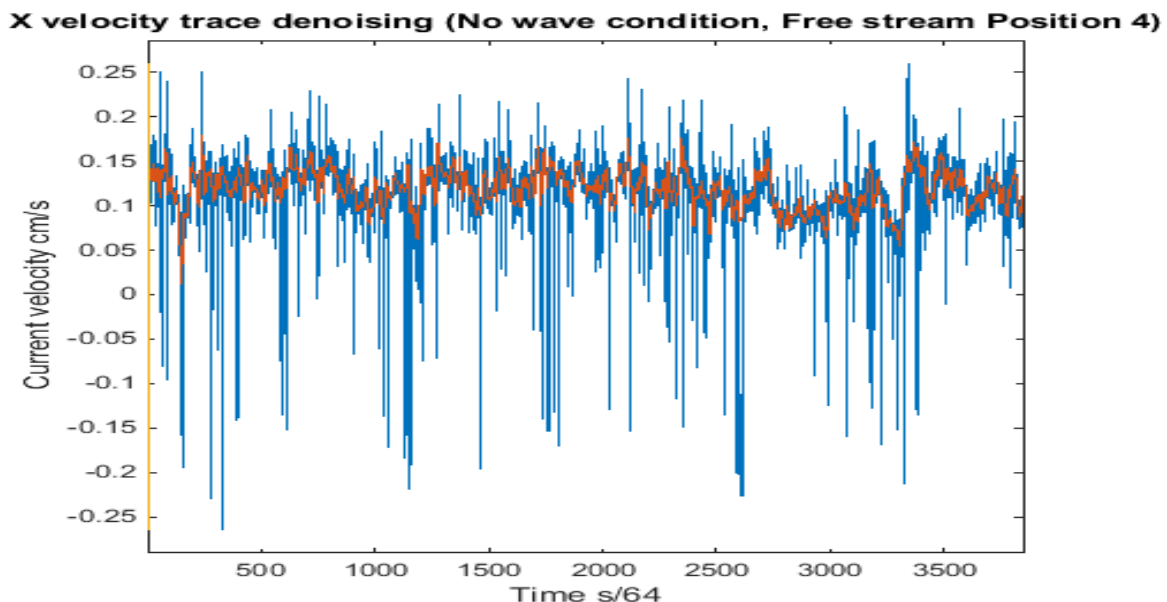


Figure 5 - Example denoised current only ADV X velocity traces (Blue - Original, Red - Denoised)

Figure 5 shows an example of the denoising process used on the data. In this trace it is probable that seeding levels were too low hence a large amount of spikes occurred. Comparing the original trace to the denoised trace to check the accuracy of the denoising was important to make sure none of the natural fluctuations in the

turbulence were affected and only false spikes were removed. In this process an element of subjectivity is present as the size of the moving average filter has a larger effect on the dataset; it was deemed that a 9 point moving average equating to an averaged velocity over 14ms was acceptable as any large fluctuations over this time were likely to be noise on visual inspection of traces.

4.3.1 Removing wave effects from velocity traces

Lastly since most of the data collected for the experiment involved the running of waves simultaneously with currents, the removal of the wave signal was necessary in order to extract the turbulence caused purely due to the flow and not the component caused by wave movement. This demodulating of the overall velocity trace again needed to be done in matlab as it is an involved process that cannot be done manually.

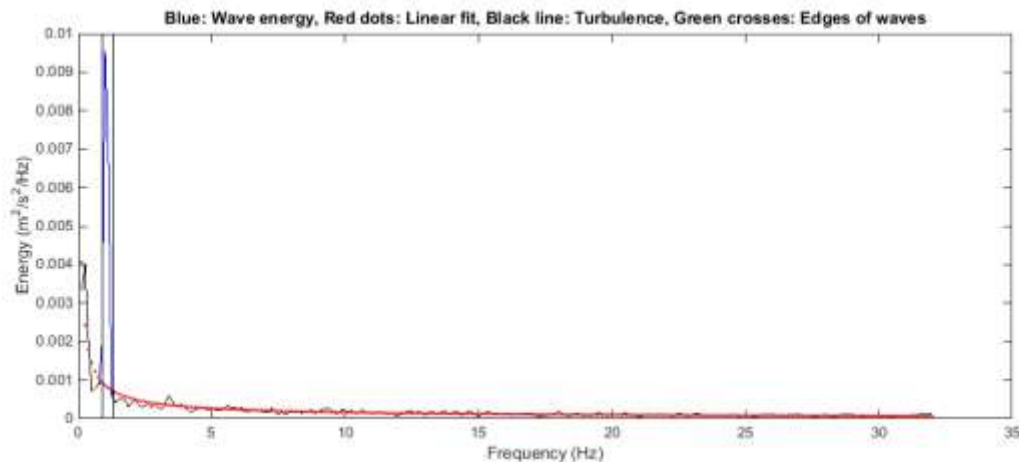


Figure 6- Example ADV Energy density plot from Vector2turb1 Matlab script Jon Miles (2003) – Data taken from Position 7 with +20 degree waves

Matlab scripts provided by Professor Jon Miles (Miles, 2003) were used to process the data based upon the Stapelton & Huntley method (Stapelton & Huntley, 1995).

Each vector velocity trace was broken down into its constituent frequencies using the Fast Fourier Transform and was represented as an energy density spectrum as shown in Figure 6. The Vector2turb1 matlab script graphically displays the frequencies across all three channels as three different colour traces and consequently any narrow banded energy spikes are clearly visible. Such spikes are then manually removed by choosing maximum and minimum frequency thresholds in order to isolate them, as displayed in Figure 7. Each of the channel's energy spectrums was then plotted on a ln/ln scale allowing the programme user to visually see if the user chosen frequency thresholds have isolated the chosen frequency in multiple channels. A linear relationship exists within the dataset of frequencies and any major narrow banded dedications can be easily seen in Figure 7 as deviating from this. Having previously chosen frequency thresholds it is possible to see if these thresholds were correct by isolating wave frequencies and motions across all channels (noting that vertical and horizontal traces are more likely to be affected than lateral frequencies).

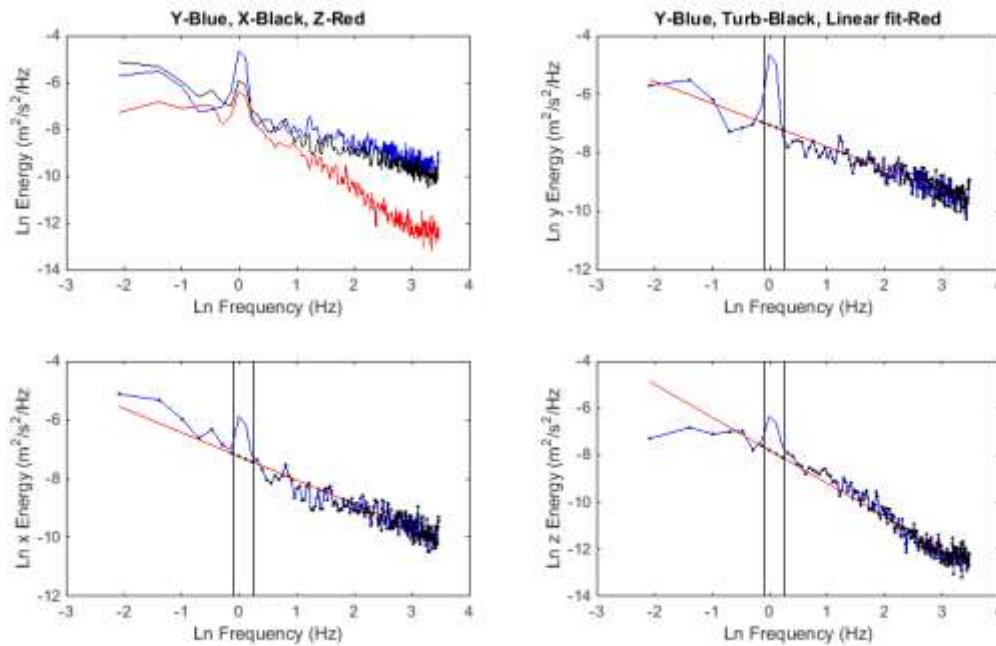


Figure 7 - X, Y & Z Ln Spectral Energy density plots showing removed wave frequency bands – Data taken from Position 7 with +20 degree waves

Theoretically it should be easy to identify the wave frequencies as the wave machine only produced one narrow band of frequency so it shows clearly in the analysis, however due to the nature of turbulence multiple peaks on the energy density graph plots were commonplace. This in turn may lead to limitations within the derived data; however this is discussed in 5.2.3 ADV wave component removal via matlab.

The matlab script then proceeds to transform the energy spectrum after removing the traces associated to the narrow peaked wave frequencies in the energy density diagram leaving velocity traces that are unaffected by the wave motion. From this denoised and processed data TKE was then calculated and has been recorded for analysis.

4.3.2 Bed shear extraction

ADV X Axis (parallel to current propagation) velocity readings were taken along the downstream Centre Line (CL) of the Monopile, readings were taken over the full range of the sensors profile instead of at a central point as with the TKE readings. The Measurement profile of 35mm was split into 35 bins consisting of individual velocity traces within each bin. Traces were recorded over 60 seconds to take into account turbulence fluctuations. Plotting a mean velocity for each bin against its corresponding height from the bed gives a linear relationship within the log layer (0 to 35mm from bed). In order to only sample within this layer data was excluded towards the top of the sampling profile as it was outside the log layer thereby keeping the R^2 value of the line of best fit above 0.9 to ensure a strong relationship as seen below in Figure 8.

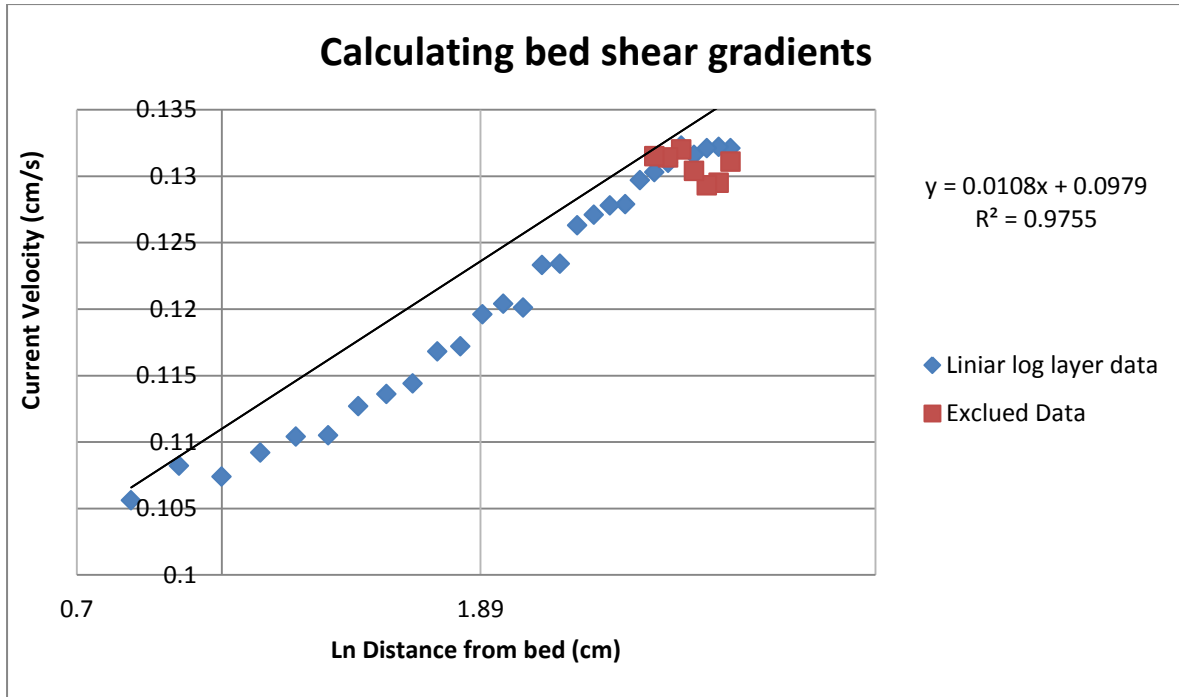


Figure 8 - Calculating Bed Shear m (du/dz) values

$$\tau = \rho u^{*2} \quad (\text{where } u^* = m \times k)$$

[2]

Equation 2 - Calculating Bed Shear Stress in log layer (Crone, No date)

Equation 2 was then used to acquire a final bed shear stress: fluid density ρ was taken at 1000kg/m^3 , k VonKarman's constant taken at 0.4 (Crone, No date) and m as the gradient from the above plotted profile of current velocities. The gradient m was taken from the gradient of Figure 8, any sensor readings that failed to gain an R^2 of 0.9 or over after manipulation were excluded from the final results as no meaningful bed shear values can be drawn from such data. This was only observed at position 2 at 0 degrees of wave propagation and was assumed to be caused by excess turbulence/phase wrapping. It was not possible to denoise bed shear force data due to the incredibly large volumes of data from all the bins, so raw velocities were used for calculations. This has been deemed to have minimal effect on accuracy due to the averaging of velocity traces of each bin.

5.0 Results of lab experimentation

5.1. Discussion of data

In total 184 TKE readings and 24 bed shear readings were taken and assessed in the wake region of the Monopile at bed and free stream depths. Results are presented in the following sections after their limitations are discussed in order to validate the data's accuracy.

5.2. Data Limitations

There are a few limitations to the data collected however they fall into two different groups: firstly limitations in the accuracy of the data recorded and secondly limitations of the data produced in terms of scalability from the prototype to the model. The first group had a direct effect on the quality of the results however the second group only limits the comparative uses of data when trying to relate experimental results back to findings at Scroby Sands. This in itself does not undermine the experimental results it only means conclusions are more standalone rather than accurately relatable to the prototype site.

5.2.1 Data accuracy limitations

The most common issue encountered in lab testing was the seeding levels in the basin which need to be monitored on a regular basis as they could quickly drop off as seeding settled or was filtered out.

Secondly, the wave gauge data was interrogated to ensure that the waves were of the correct specified scale otherwise further assumptions drawn from this data would not be meaningful. Of the nine wave gauge readings taken over the course of the Labs it was found that four of these readings did not record, leaving only five wave traces to determine if the waves generated were of the required amplitude (which was 10mm as seen in Table 1). It was found that that waves being propagated at +20° had a mean amplitude of 10.5mm, waves of 0° had a mean amplitude of 12mm and waves of -20° had a mean amplitude of 8.5mm. This again is another limitation to the data as shown by Figure 9 below which shows a superposition of all the different wave conditions applied to the tank.

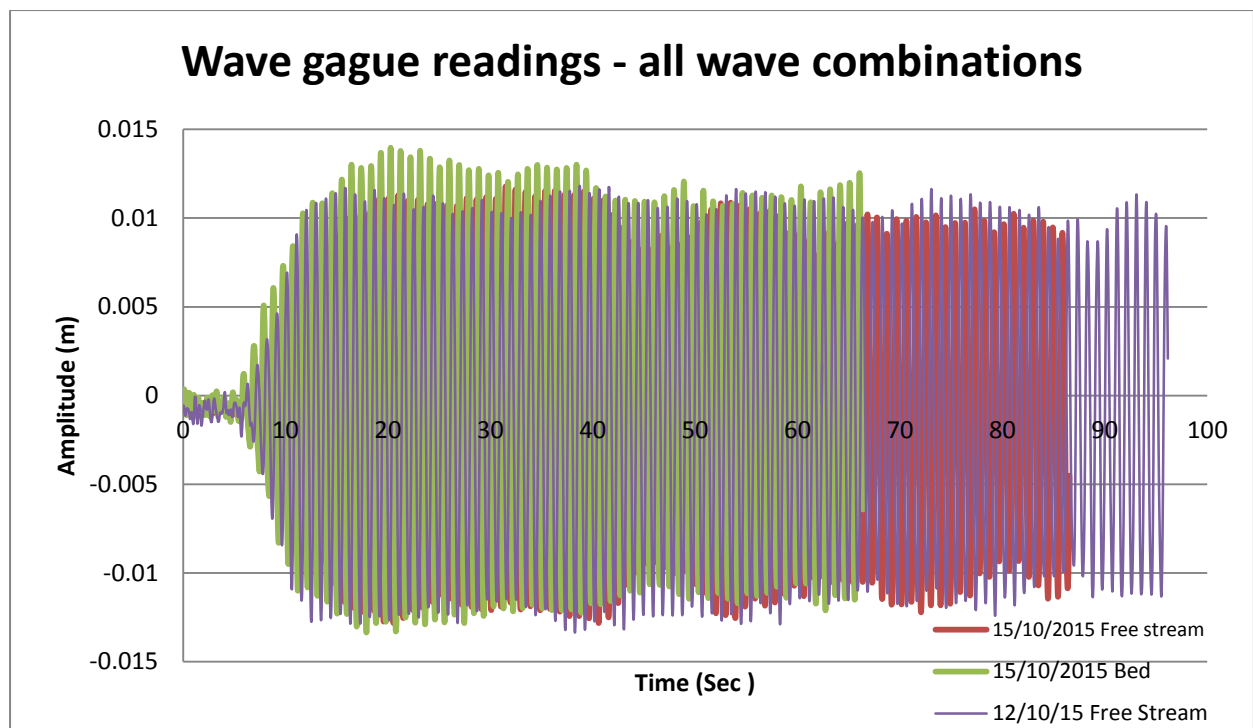


Figure 9 – Superimposed wave tests (Amplitude accuracy check) – 1cm (0.01cm) specified wave amplitude

5.2.2 Scaling issues

Lab experiments use Froude scaling over Reynolds scaling due to the gravity and inertia (from the wave and currents) being the main acting forces in the experiment. When parameters are scaled down from prototype level to model level some scaling issues occurred which are discussed below.

As can be seen in Table 1 it was not always possible to generate the exact scaled conditions from prototype to model. The largest issue with scaling issues should theoretically come from the wavelength as the wave causes circular motions of water particles and the longer the wavelength, the deeper the wave's motion goes (e.g. Wavelength/2). Being unable to scale to the full required 1.38m wavelength may have caused a reduction in experienced turbulence however this cannot be proven without further testing.

Secondly, wave scaling in the model was required to have a wave height of 1.6cm; however 2cm was achieved. This cannot be avoided as it is purely a limitation of the wave paddles. Two further scaling conditions need to be fulfilled in order to avoid scaling effects from surface tension; water depth over 2cm and wave periods over 0.35Hz. Both of these conditions were achieved therefore surface tension effects were negligible in the experiment so will not be discussed further.

Lastly, the density of the water must be mentioned as in the prototype the seawater density would be around 1025kg/m³, however this was unachievable in the lab as the basin was filled with fresh water of density 1000kg/m³. This is not accounted for in scaling calculations and cannot be changed due to practicalities. This scaling issue consequently means that accuracy is lost when scaling lab results from model to prototype however this is not the largest source of inaccuracy.

5.2.3 ADV wave component removal via matlab

This manual identification of the frequency thresholds adds a level of subjectivity to the results which may affect the accuracy of post processed results. In cases such as Figure 6 & Figure 7 where one peak is clear the peak is easily detected and accurately removed. However in the case where there are multiple frequency peaks accuracy may be lost in selecting frequency thresholds. Sadly this is unavoidable as the processing of results is done by hand when setting thresholds so no improvement can be made here. Since all results have undergone this process it is a repeatable error so all results have the same level of accuracy.

5.3. Observations

5.3.1 Analysis of wave propagation angles on TKE distribution

Results have been processed in terms of % Environmental impact (%EI) as shown in Equation 3, this has been done in order to make clear and simple comparisons between data collected under pure current conditions and that collected under current and wave conditions.

$$\text{Environmental Impact } EI (\%) = \frac{(X_{After} - X_{Before})}{X_{Before}} \times 100 \quad [3]$$

Equation 3 - Determine %EI from TKE data

A table detailing all of the %EI values in both bed and free stream positions can be found in Appendix 4.0 and should be referred to with reference to the sensor position map in Appendix 3.0. This information has been refined and important elements have been graphically depicted in order to communicate findings more clearly.

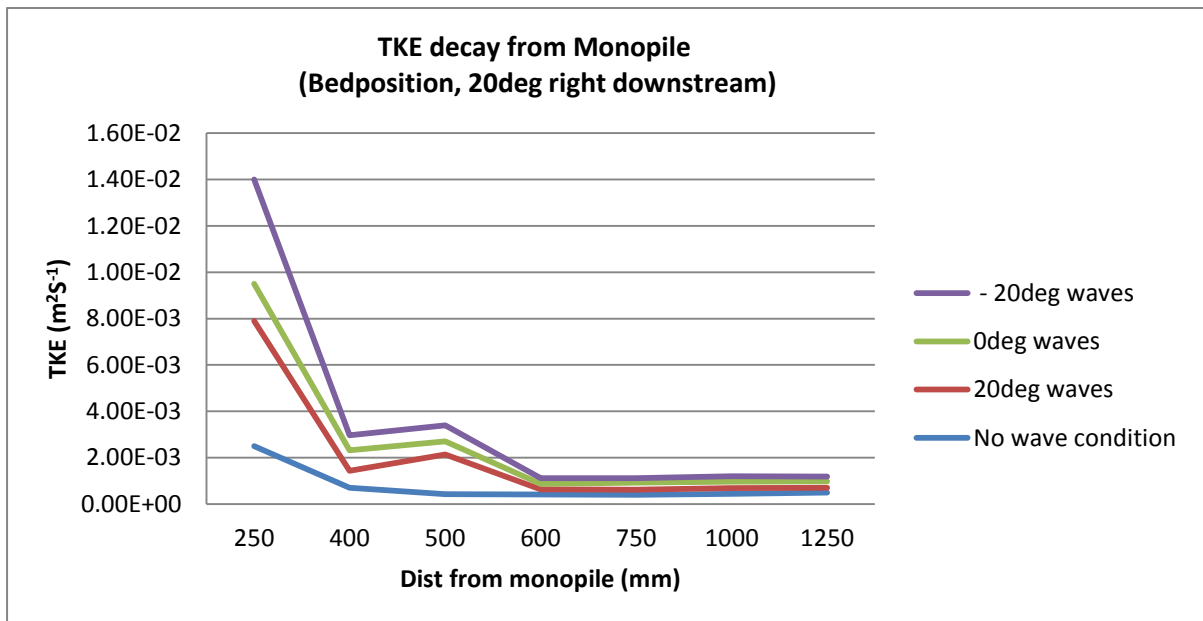


Figure 10 - TKE decay in bed position along a transect 20 degrees right of the downstream centreline behind the pile

Figure 10 depicting the right 20 degree downstream transect shows there is a clear correlation between all the wave data sets with a similar pattern repeated in each experiment, albeit indicating raised energy levels compared with the current only situation. Amongst the readings there was a uniform drop in TKE along the right hand transect at a distance of 400mm from the Monopile, the TKE then rises slightly to a peak at around 500mm. Past 500mm TKE can be seen to decay back to background levels indicating sample locations are outside the Monopiles wake region. TKE traces vary in their energy levels between angles of wave propagation with negatively angled incident waves having a larger TKE values. This agrees with common thought that when currents and waves are propagating in similar directions TKE will be higher.

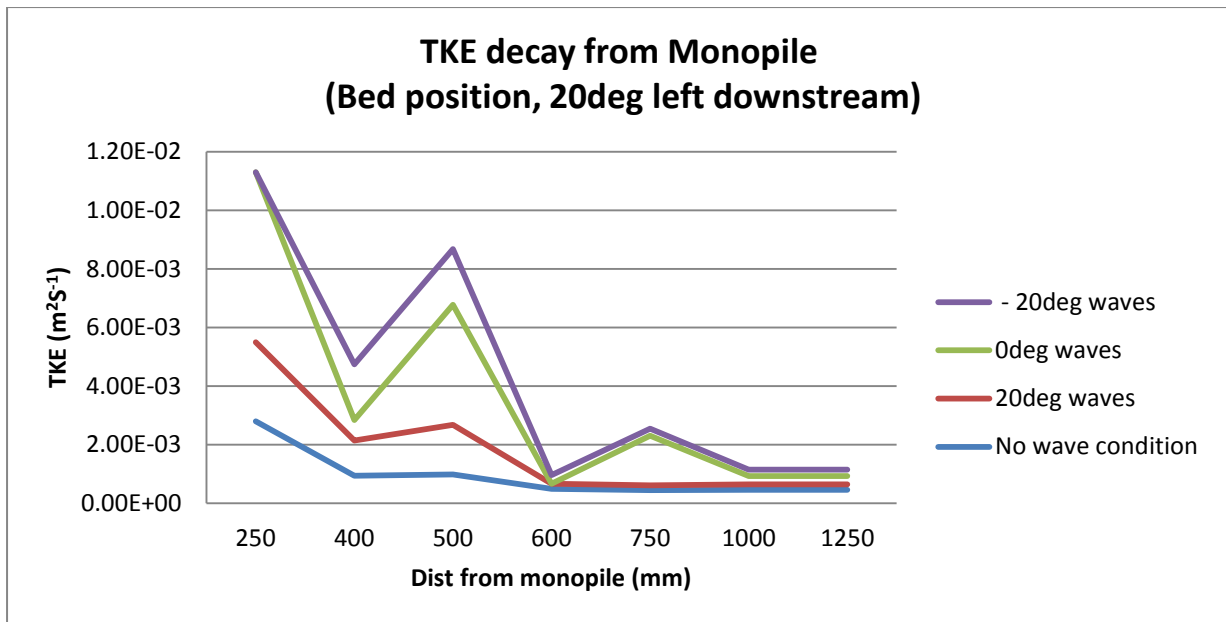


Figure 11 - TKE decay in bed position along a transect 20 degrees left of the downstream centreline behind the pile

Figure 11 showing the left 20 degree downstream transect shows a larger spread of TKE between locations indicating the presence of a wake region; this logically makes sense as the wake region is likely to have shifted away from the wave generator side in the wave tank depicted in Appendix 2. The presence of the wake region is assumed to die out at a distance of 1000mm from the Monopile. Similarly to Figure 10 the same spike in TKE is observed at 500mm from the pile experienced under all wave conditions however with an additional peak at 750mm experienced by only - 20deg and 0deg waves possibly due to the smaller incidence angles of the waves.

Comparing the edge of the wake region in Figure 10 & Figure 11 it can be seen that the extent of the wake region varies, this indicates the rotation/movement of the wake itself under wave action. Comparing the distance from the Monopile to background TKE levels shows the wake region has rotated left (anticlockwise) of the Monopile which is furthest from the origin of the wave propagation.

Results indicate the magnitude of TKE for differing wave angles remains the same along both transects with negative angles alluding to higher levels of TKE compared to positive angles because of the aligning of waves and currents.

Comparing the spikes in TKE at distance from the Monopile along both transects, it can be seen that peaks of TKE occur at 250mm & 500mm, 700mm with troughs at 400mm and 600mm. For free stream graphs and results, please refer [4] the "Preliminary Results" excel file on the attached CD annex.

$$\text{Reynolds Number } Re = \frac{uD_p}{\nu}$$

Equation 4 - Reynolds number calculation from a Monopile in a current (Dight, 2013)

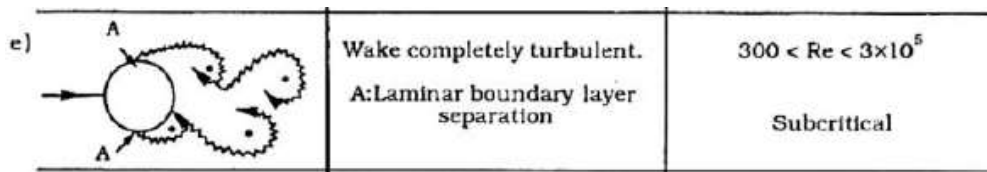


Figure 12 - Vortex patterns from Monopiles in currents (Sumer & Fredsøe, 1997)

Sumer & Fredsøe predicted this series of peaks and troughs in Figure 12 from the calculated Reynolds number of $1.6E+4$ from Equation 4 (further referenced in Project I) compared to the patterns in the above graphs (Sumer & Fredsøe, 1997). It can be seen that a similar pattern of TKE peaks and troughs occur along both transects from the Monopile further validating the experiments set up and validity of results.

5.3.2 Analysis of TKE decay downstream of the Pile

The decay of TKE downstream of the Monopile has been taken along the downstream centreline (CL) from the Monopile, this has been done as a purely comparative exercise as the directional shape of the wake region changes slightly due to the angle of wave propagation as demonstrated from the above results. Any readings taken along the downstream centreline from the Monopile will still fall within the wake region so can be used for comparisons between differing angles of wave propagation tests.

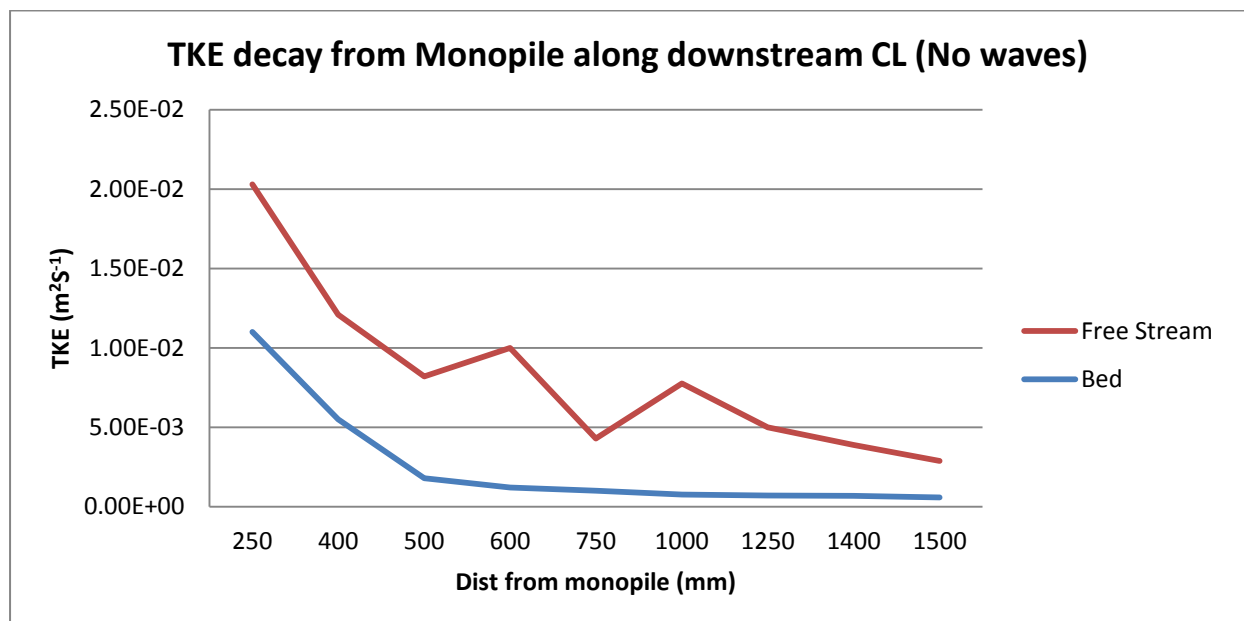


Figure 13 - Decay of TKE from Monopile in bed & free stream positions downstream of Monopile CL

Figure 13 shows the decay of TKE under a current only condition and how it differs between bed and free stream locations. As can be seen more TKE can be observed at free stream level compared to that at bed level. Free stream TKE can also be seen to fluctuate in its decay compared to that of bed TKE which follows a smoother decay. The maximum peaks experienced in the free stream TKE trace behind the Monopile CL correspond with TKE maximums along the plus and minus 20 degree

(left and right) transects. This indicates the presence of vortices in behind the downstream wake region corresponding to Figure 12.

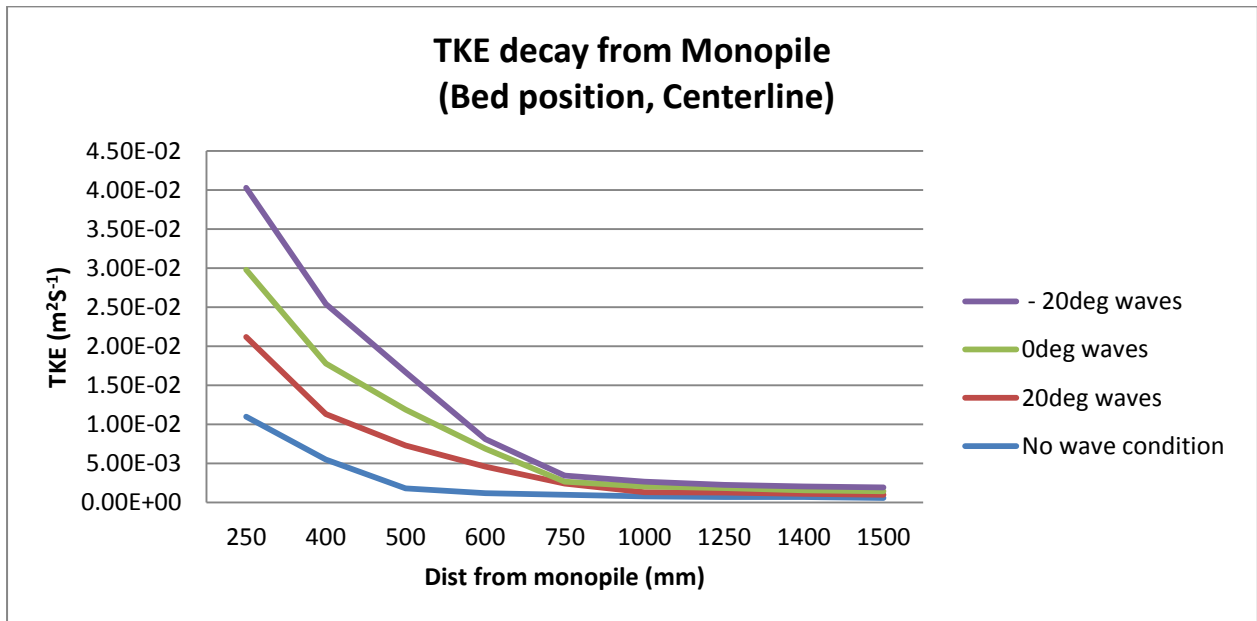


Figure 14- Bed Position TKE along a transect downstream behind Monopile CL

Figure 14 shows bed TKE under the experience of waves, it can be seen that TKE levels smoothly decay along the downstream Monopile CL regardless of wave activity. It can be seen that due to the depth of such sample locations wave action and turbulent vortices had little effect on TKE levels above the bed unlike bed TKE readings along the +/- 20 degree transects.

As with the TKE measured along the transects it can be seen that the more negative the wave propagation angle the more TKE is experienced due to the aligning of the waves and the current. The rate of decay of negative wave angles is much higher than that of positive angles from its higher initial level of TKE back to background levels as shown by the steeper decay profiles on the graph.

It can be roughly estimated that in the bed position TKE levels fall to background levels at roughly 800-1000mm downstream of the Monopile, this is similar to that observed in Figure 11 and denotes the extent of the turbulent wake region.

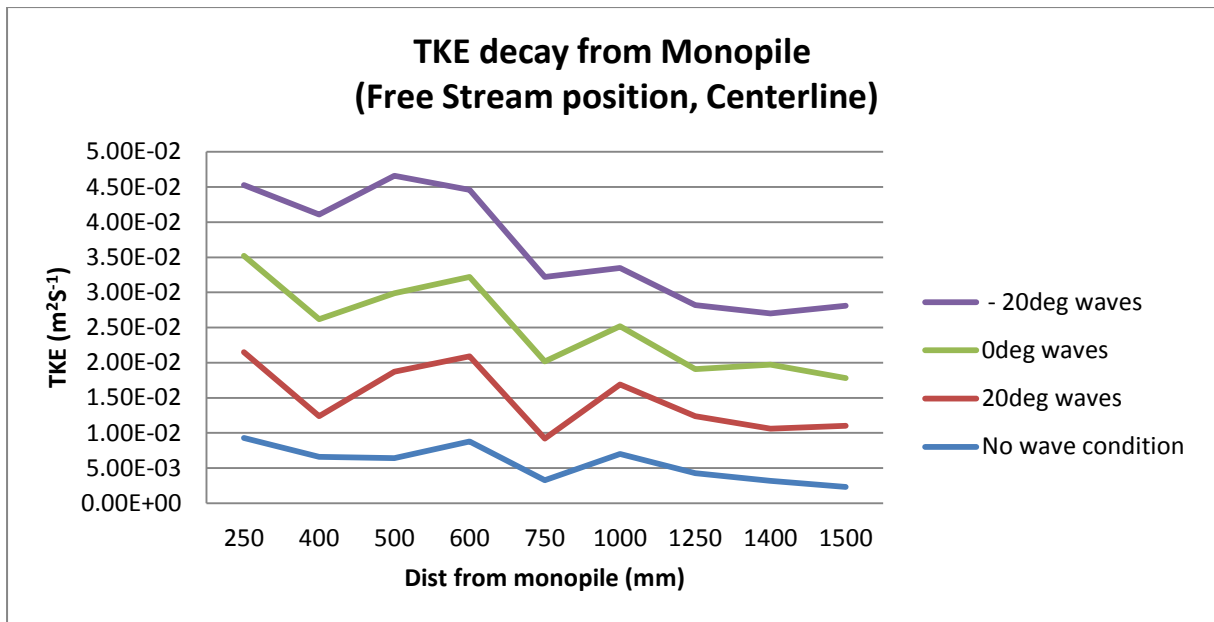


Figure 15 - Free Stream Position TKE along downstream transect behind Monopile CL

Figure 15 shows the same downstream CL TKE decay behind the Monopile, it is clear that unlike the bed position decay in the free stream is not a simple decay but is affected by turbulent vortices resulting in peaks and troughs. The same pattern emerges showing that negative angles of wave propagation result in higher TKE levels in the wake region as shown by the vertical separation of TKE traces. Secondly the extent of the wake region appears to extend to around 1400mm before a flattening of the trace can be identified, comparing this to that in Figure 14 it can be concluded that turbulence in the free stream decays around 60% slower than that at the bed level.

TKE peaks on the traces again occur at around 1000mm downstream of the Monopile, comparing these peaks to right and left +/- 20deg transects it can be seen that troughs can be found along the transects at corresponding locations indicating a turbulent vortex has formed along the downstream centreline of the Monopile.

TKE has been scaled from model up to prototype level. This has been done to enable a comparison of lab measured bed shear results and TKE inferred bed shear results at prototype scale. Such results are then compared to bed shear results taken at the prototype site of Scroby Sands in order to compare magnitude and discuss applicability of modelling.

5.3.3 Analysis of bed shear stress downstream of the Pile

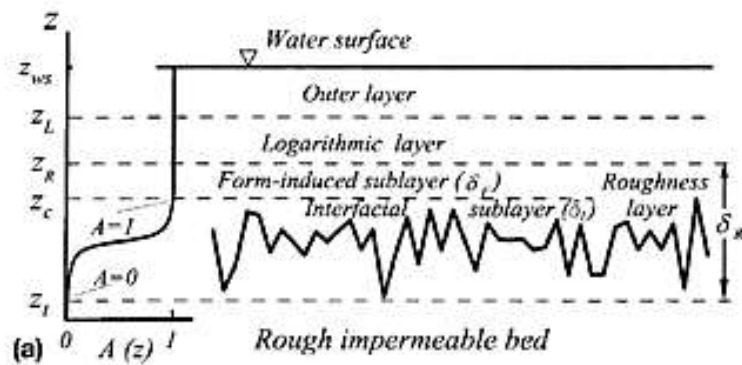


Figure 16 - Diagram of layers within a flow (University of Illinois, No date)

Bed shear was directly observed at 6 positions along the downstream centreline of the Monopile at distances ranging from 600mm 1500mm. Bed shear was then calculated using Equation 2 and plotted onto Figure 17 and consequently conclusions were drawn. When extracting the bed shear from the ADV data a strong linear relationship was observed within the “log layer” of the flow, this was clear from around 0 to 3.1 cm before becoming nonlinear as seen in Figure 8. It must be noted that only bed shear in the direction of the downstream direction of the current was observed as it was determined to be the most likely direction to experience bed shear.

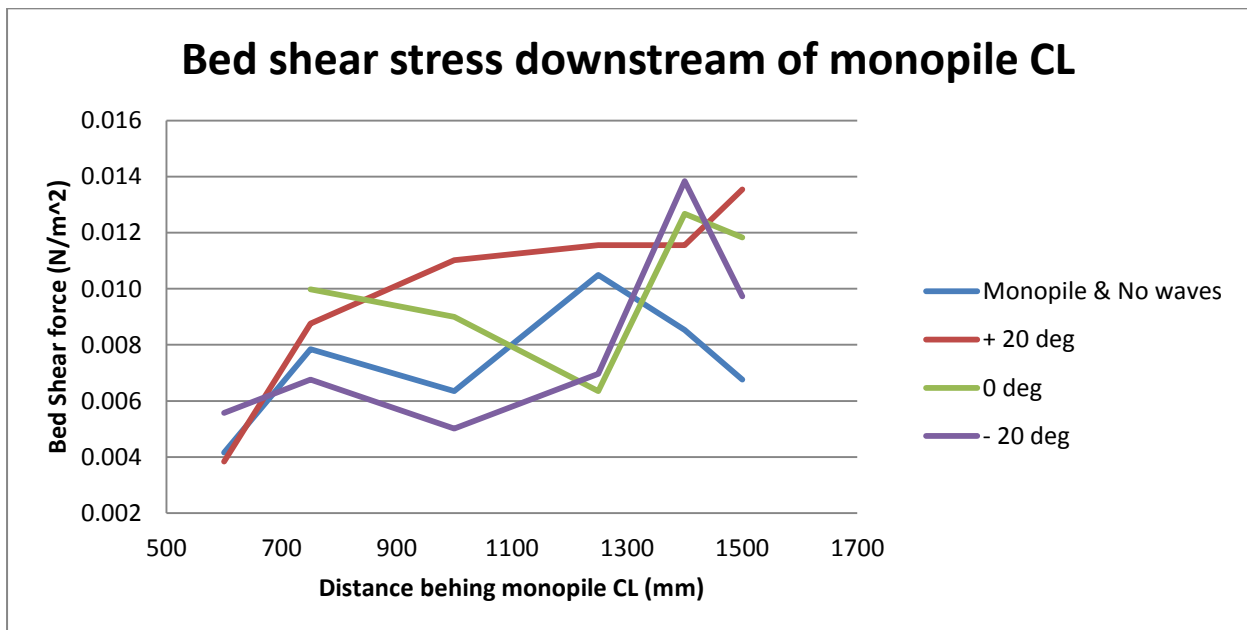


Figure 17 - Observed bed shear downstream of Monopile CL

As can be seen the angle of wave incidence angle has an effect on the magnitude of downstream bed shear Stress, however relationships are not as clear-cut as in the above section when dealing with TKE.

A number of conclusions can be drawn from Figure 17:

- Comparing background levels of bed shear with and without the presence of a Monopile in a current only condition shows the presence of a Monopile reduces levels of bed shear overall. Without a Monopile the generic bed shear stress levels was recorded at 0.020 N/m^2 which is notably higher than all of the above readings in Figure 17. A potential reason for this is that the presence of a wake region disturbs uniform flows leading to lower velocity averages being witnessed over the relatively long 1 minute sampling period.
- At distance 600mm from the Monopile all traces except the 0deg waves can be seen to experiencing a minimum value, possibly indicating it is in a location in the lee of a vortex therefore experiencing low current.
- The +20deg wave propagation bed shear profile shows clear growth with distance from the Monopile, this can be attributed to the growing influence of the waves and current interacting at large angles causing a higher level of bed shear stress.
- A peak in bed shear stress can be observed for 0deg and -20deg waves at 1400mm from the Monopile again possibly caused by vortex action.
- At 1500mm from the Monopile -20deg and no waves both troughs indicating the position lies in the lee of a vortex under such conditions.

Prototype bed shear readings (N/m^2)					
Sensor number	Distance downstream of Monopile CL (m)	Monopile & No waves	Monopile & Waves		
			+ 20deg	0deg	- 20deg
2	30	0.2081	0.1921		0.2785
5	37.5	0.3920	0.4381	0.4993	0.3380
8	50	0.3175	0.5511	0.4500	0.2509
11	62.5	0.5249	0.5780	0.3175	0.3485
14	70	0.4263	0.5780	0.6337	0.6919
16	75	0.3380	0.6771	0.5917	0.4867
Min Bed Shear (N/m^2)		0.1921			
Max Bed Shear (N/m^2)		0.6919			

Table 2 - Bed Shear Stress Measured and scaled to Prototype level

Particle classification name	Range in particle diameter (mm)	Critical bed shear stress (τ_c) (Nm ⁻²)	Critical shields parameter (θ) (dimensionless)
Coarse cobble	128-256	112-223	0.054-0.054
Fine cobble	64-128	53.8-112	0.052-0.054
Very coarse gravel	32-64	25.9-53.8	0.05-0.052
Coarse gravel	16-32	12.2-25.9	0.047-0.05
Medium gravel	8-16	5.7-12.2	0.044-0.047
Fine gravel	4-8	2.7-5.7	0.042-0.044
Very fine gravel	2-4	1.3-2.7	0.039-0.042
Very coarse sand	1-2	0.47-1.3	0.029-0.039
Coarse sand	0.5-1	0.27-0.47	0.033-0.029
Medium sand	0.25-0.5	0.194-0.27	0.048-0.033
Fine sand	0.125-0.25	0.145-0.194	0.072-0.048
Very fine sand	0.0625-0.125	0.110-0.145	0.109-0.072
Coarse silt	0.031-0.0625	0.0826-0.110	0.165-0.109
Medium silt	0.0156-0.0310	0.0630-0.0826	0.25-0.165
Fine silt	0.0078-0.0156	0.0378-0.0630	0.3-0.25

Table 3 - Partial shear (USGS, 2008)

Comparing calculated prototype level bed shear forces in Table 3 and critical bed shear forces in Table 2 it can be seen that medium to very coarse sand is susceptible to becoming dislodged from the bed within the downstream wake region.

A comparative prototype level bed shear stress comparison was undertaken relating the above scaled model bed shear stresses to prototype level in order to compare lab obtained results with measured results taken at Scroby Sands. Data was scaled using Vassalos rules for stress Scaling (Vassalos, 1999) from model to prototype level and compared against both hypothetical bed shear stress results obtained from the TKE testing using a scaling technique from the University of Illinois (University of Illinois, No date) and the above observed bed shear stresses. Bed shear stress results from both experiments can be found in Appendix 5.0.

5.4. Summary of Results

Angle of wave incident effect on wake region shape

- It was found that the wake region rotated anticlockwise away from the wave generator under more negatively angled incident wave conditions.
- TKE maximums and minimums were experienced at similar locations along left and right downstream transects from the Monopile.
- The presence of waves increased TKE levels in the wake region with more TKE occurring under negative wave propagation angles.
- Higher levels of TKE were experienced at free stream level compared to that measured at bed level.

Angle of wave incidence effect on wake TKE decay

- Higher levels of TKE were experienced at free stream level compared to that measured at bed level.
- A larger number of TKE fluctuations are experienced at free stream level due to the presence of vortices.
- The presence of waves increased TKE levels in the wake region with more TKE occurring under negative wave propagation angles. The more negative the angle the faster the decay of TKE to background level at bed level.
- Uniform background TKE levels for all wave conditions at bed level were measured for all wave conditions whereas at free stream each wave condition had its own decayed TKE background level.

Angle of wave incidence effect on wake shear stresses

- The presence of a Monopile decreases the amount of bed shear experienced compared to the background level of bed shear stress with no Monopile in a current only situation in the 1 minute sampling period.
- The angle of wave propagation has an effect on the bed shear stress experienced possibly due to the changing of vorticity positions and varying current velocities leading to no clear-cut relationships.
- Large angles of wave propagation +20deg have a consistently higher level of Bed Shear than other wave propagation angles.

6.0 Discussion of findings

6.1 TKE distribution in Wake Region

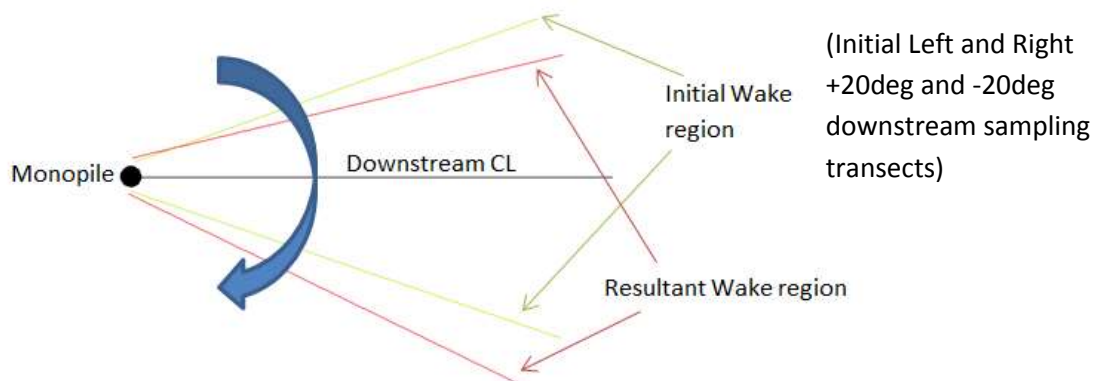


Figure 18 - Rotation of wake region under negatively angled propagated waves (originating at top of diagram)

The above conclusions indicate with a high level of certainty that the wake region has rotated under the presence of negatively angled waves due to the difference in TKE decay between the right and left transects. This is demonstrated in the above Figure 18 showing how the movement of the wake can result in the unbalancing of the TKE experienced along the initial wake position (left and right transects assumed to be within the initial wake region – green lines). In the presence of 0deg and -20deg waves the wake region rotates to the red line position resulting in a drop in

TKE at distance along the initial right hand (top) sampling transect and a rise in TKE along the left hand (bottom) transect.

The wake region is composed of turbulent water making it hard to define due to the presence of moving vortices along the edges of the wake region as demonstrated in Figure 12. In order to better understand the development of the wake region under differing angles of wave propagation and a much denser net of sampling points is needed in order to more accurately define the limits and development of the wake region. A denser sampling grid would also allow a feather plot to be produced to better define turbulence and vortex features in the wake region (in plan view) helping to understand the movement and evolution of flow patterns in the wake region.

Another issue with conclusions drawn in regards to movement of the wake region is the potential for limited transferability of results due to the fact that testing was only undertaken under one current and wave condition. It is reasonable to assume that the wake will rotate as above under negative wave propagation (when wave propagation direction is more aligned with that of current direction) however this rotation will be severely affected by the velocity of the current and the size and period of the waves. For this reason no statistical conclusions have been derived. Wake rotation in reference to the Prototype site of Scroby Sands cannot be confirmed with the available data as no detailed long term TKE assessments with a similar setup have been undertaken.

6.2 Wake Region TKE decay

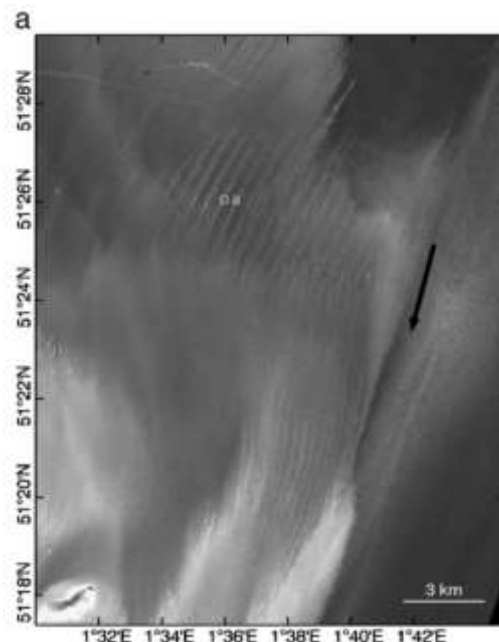


Figure 19 - Turbid wakes from Thanet OWF as viewed from Landsat 8 (Vanhellemont and Ruddick, 2014)

As seen in all of the graphs in section 5.3.2 a clear decay in TKE along the downstream CL of the Monopile is seen following a gentle decline. Again higher

levels of TKE were noted for negative angles of wave propagation compared to positive angles at both bed and free stream levels. Within the analysis of downstream TKE decay in the experiment differing conclusions from bed level decay and free stream level decay were seen.

At bed level TKE was seen to decay smoothly as seen in Figure 14 with negative angles of wave propagation resulting in higher levels of TKE compared to that of positive angled waves. TKE was seen to decay faster for such negatively angled waves whereby all wave and no wave conditions had decayed to equal background levels of TKE at around 800mm or 8 Monopile diameters downstream of the Monopile. At bed level it is acceptable to assume currents are the main influence of TKE decay and waves have little effect in this region.

At free stream level it was observed that a similar TKE decay to background levels occurred at around 1400mm from the Monopile as seen in Figure 15 however with decays featuring troughs and peaks most likely associated to vortices in the wake region. At free stream level it is harder to define if waves or currents are an influencing factor when it comes to TKE decay as each wave propagation angle holds its own distinct TKE level. It is also unclear if the wave propagation angle affected the decay and position of the vortices as again only one current and wave scenario was modelled. In order to compare the movement, evolution and decay of such eddies at free stream height, multiple current and wave conditions need to be run and compared in order to determine if the waves affect the movement/decay of vortices in the free stream.

For both bed and free stream data the clarity of established relationships is quite clear in the wave and current conditions experienced in the laboratory. However from the undertaken lab testing it is unclear if the distance for TKE to decay to background levels of 8 Monopile diameters (bed level) / 14 Monopile diameters (free stream level) will still apply in other current and wave conditions.

It would be logical to assume a continued relationship like this at bed level due to the lack of wave interaction/effect not causing peaks and troughs in TKE as seen at free stream level, however this would need lab testing to clarify. At free stream level the relationship is not as clear-cut as each angle of wave propagation has its own background TKE level as seen in Figure 15, however it can be seen that all traces reach their own assumed background level at around 14 Monopile diameters downstream of the Monopile. The transferability of such results under different wave and current conditions is questionable due to the changing Reynolds number and consequent differing vortex pattern downstream of the Monopile as described in Figure 12 by Sumer & Fredsøe.

From the TKE decay traces it would be logical to assume that of the two patterns the smooth decay curve of the bed level TKE would be present in other current and wave scenarios due to the fact it is not affected by the changing Reynolds number or turbulent eddies. This said, the extent of the wake region cannot be predicted from this work due to only one wave and current criteria (Scroby Sands at model level) being tested in other current/wave conditions so the 8 Monopile diameters will not apply. It can safely be assumed that the faster the current conditions the larger the

wake region will extend downstream of a Monopile and will yield a potential for more scour within the wake region however further research is required in this area to substantiate any such predictions.

Lastly as seen in Figure 19 turbidity wakes can be seen formed downstream of the Monopile, this feature is caused by turbulence keeping sediments in solution. Decay of TKE in the free stream is a major factor in these wake regions as turbid wakes can stretch for several kilometres (Vanhellemont and Ruddick, 2014). The lab work sadly does not present any conclusions about turbid wake decay due to the fact the experiment was scaled to focus on inter-array TKE so is consequently too small to draw conclusions from in this case.

6.3 Downstream bed shear stress

As seen in Figure 17 and stated in the above section 5.3.3 bed shear stress was hard to draw many clear-cut conclusions from the data as was the case with TKE experiments.

$$TKE = K \Rightarrow \tau_b = 0.19K\rho \quad [5]$$

Equation 5 - Inferring Bed Shear Stress from TKE equation (University of Illinois, No date)

A comparison between the bed shear stress values derived from empirical lab testing and those inferred through TKE testing and the TKE to bed shear Equation 5 (where $\rho = 1000\text{kg/m}^3$) was undertaken and can be found in Appendix 5.0. Comparing the two it can be seen that there is a definite difference in magnitude between observed and inferred results ranging between 5 to 185 times as large as the directly measured ones (for calculations please see the table of calculated differences found in the *Preliminary Results* excel sheet in the CD annex). There was no common trend or scaling factor found in this comparison which in the context of this work does not lend credibility to the TKE inferred bed shear stress relationship.

In the undertaken work there are a number of potential limitations in the way bed shear data was collected and processed. Firstly bed shear stresses were only calculated from X (downstream) current components and did not take account of the Y (cross stream) component of flow to take an aggregate bed shear stress. This has limited the accuracy of results obtained as it is hard to accurately describe a two dimensional process when only a one dimensional analysis has been used. This has limited the accuracy of the bed shear stress results obtained. This said the majority of higher velocity flows will have occurred in the X direction due to the direction of the current propagation but the size of perpendicular currents caused by potential eddies cannot be determined so may have had a large effect on results.



Figure 20 - Fluid turbulence shown using dye tracer (Tumbler, No date)

Secondly bed shear stress samples were only collected along the downstream centreline from the Monopile, this positioning of data collection points when compared to Figure 12 shows the downstream centreline from the Monopile to be in a somewhat sheltered position and avoiding most of the turbulence caused on either side of centreline. The assumption here being that higher flow velocities would be experienced in the fluid within a region of eddies compared to being in the relatively sheltered area behind the Monopile. Again this could be solved by a much denser net of data collection points ideally with some within in the wake region immediately downstream of the Monopile.

Thirdly the sampling period of results may have been a hindrance to the data collected. A sampling period of 60 seconds was used. It is thought that the averaging of the velocities in all bins across this 60 second interval could have vastly underestimated the maximum velocities in each bin therefore underestimating the maximum shear experienced. Bed shear was assessed in order to draw conclusions about scour downstream of the Monopile however only average shears were assessed. In the case of a sampling point in the middle of a moving vortex shed from the Monopile the 60 second average bed shear will not best represent the maximum scour potential. This being the case shorter sampling periods would be suggested in order to achieve a more representative analysis of bed shear stress potentially focusing on maximums obtained from a number of tests to best represent shear bed stress in the wake region.

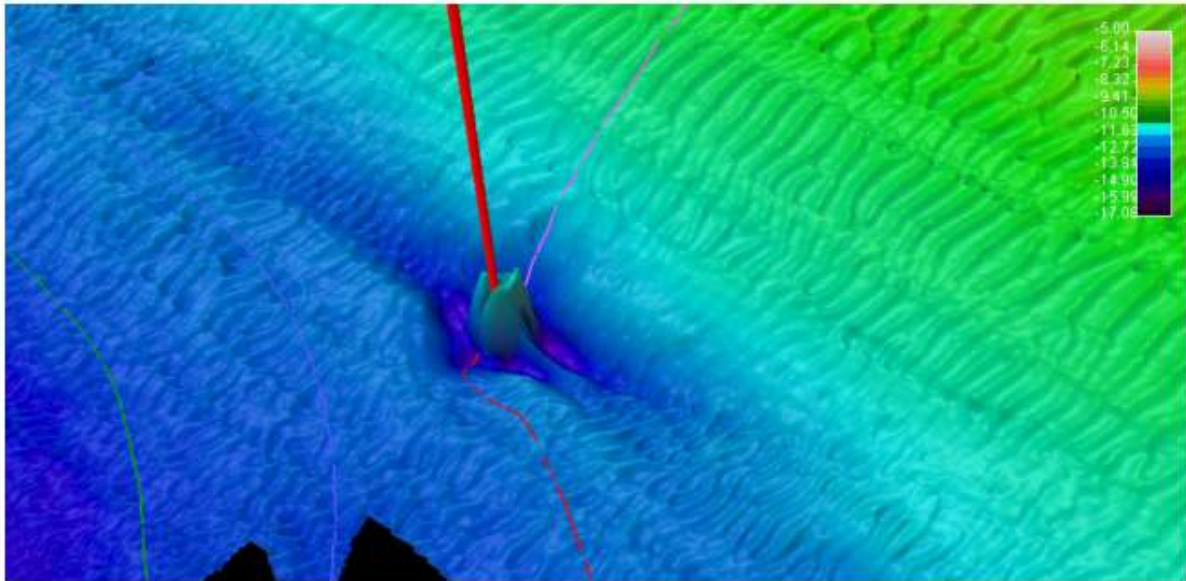


Figure 21 - Fledermaus image showing the scour protection around the base of the monopile (red cylinder ~4.2 m diameter, WTG01), along with the secondary scour pits and the "as laid" intra-array cable route (magenta line) and the export cables (red and green lines).

Figure 21 - Scroby Sands Monopile bathometric scan of wake region showing scour pit (CEFAS, 2006)

Comparing experimental laboratory bed shear stress data that has been scaled up from model to prototype level against observed bed shear results taken at the sample site of Scroby Sands revealed a close correlation in the scale of the numbers obtained. Directly measured and scaled results taken from laboratory testing ranged from $0.19 - 0.69 \text{ N/m}^2$ as seen in Appendix 5, noting that lab testing only measured from a scaled diameter of 30m from the Monopile downstream and bed shear (along with TKE) increases with proximity to the Monopile. Bed shear stresses were measured at Scroby as part of the Environmental Impact Assessment (EIA) as dictated under European policy (Metoc plc, 2000) revealed that generic combined wave and current shear forces of between $0.4 - 1.2 \text{ N/m}^2$ were measured (CEFAS, 2006).

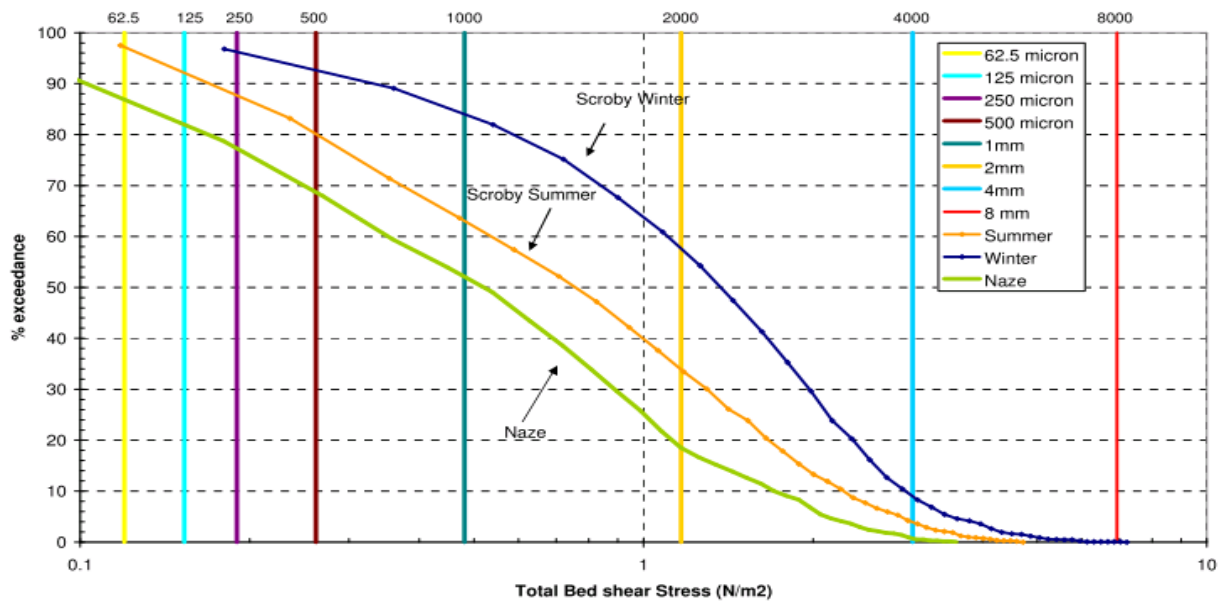


Figure 22 - Total Bed Shear Stress exceedance in Summer and Winter for various particle sizes

This comparable bed shear stress indicates that the wave and current parameters were scaled correctly. The fact it is on the low side of the scale reflects the fact the readings have been taken along the downstream centreline where less turbulence is experienced as discussed above. During the winter storms at Scroby it was noted in the Environmental Impact Assessment (EIA) that shear bed stresses could exceed 3 N/m² for around 10 % of the time, in the laboratory experiment typical non storm conditions and currents were modelled using a regular sinusoidal wave form and constant currents. This difference in summer and winter is reflected in Figure 22 and shows the effect on various sediment sizes affected by different hydrodynamic conditions at the site.

The waves employed in the laboratory testing were not representative of the “worst case” winter type storms experienced on the prototype site where the worst bed shear stresses and consequently sediment erosion occurs. This offers the potential for further laboratory testing in order to make a better assessment of conditions in which scour and mean bed shear stress peaks.

$$\text{Terminal velocity of partial descent } u = \frac{2(\rho_p - \rho_f)}{9\mu} gR^2 \quad [6]$$

Equation 6 - Stoke particle settling equation (Shearer, No date)

An attempt was made to derive the vertical fluid velocity from the prototype bed shear stresses using the TKE bed shear stress relationship and mathematical rearrangement of the TKE formulae. A number of very crude assumptions had to be made in order to do this, namely assuming X, Y and Z velocities are similar in size in order to infer the vertical fluid velocity. This vertical fluid velocity was then compared to the stoke equation (Equation 6) estimated falling velocity for sediment particles of an average size of 1mm as specified in the Cefas report. Again there was a scale

issue between the generic sediment falling velocity of 0.598 m/s and the predicted upward vertical fluid velocity's (0 to) $1.1\text{E-}3$ m/s at bed level stemming from the crude assumption of equally distributed fluid velocities in X, Y & Z axes. Another method was then employed to look at the upward vertical flow at the rear CL extremity of the wake region. The mean Z flow components were extracted from initial TKE data and compared and then compared to the sediment fall velocity. At prototype level it was found that the maximum upward flow velocities were $8\text{E-}3$ m/s at bed and at free stream 0.03 m/s. This theoretically meant that sediment would be deposited before the 75m mark according to the laboratory model.

The Scroby Sands EIA also observed scour wakes around 300m long and 100m wide at scoured depths of approximately 1m below the initial sea bed (CEFAS, 2006). This observed scour range indicates that deposition is not occurring in this area which is in direct contradiction to the predicted sediment deposition observed in the lab testing. There are a number of potential reasons for this discrepancy, firstly as stated earlier the downstream centreline from the Monopile where readings were taken generally witnessed less vortices. Secondly this is deposition under average non stormy conditions therefore not truly representing worst case storm conditions where there would be a more energetic hydrodynamic condition therefore encouraging particles to stay in solution rather than being deposited. Thirdly although the lab data indicates average sediment deposition in the prototype wake region it doesn't take into account long term conditions whereby the deposited sediment may have been consequently removed by a series of storm events. As can be seen there are a number of possible reasons as to why there is a discrepancy between lab data and observed prototype sediment behaviour. This again indicates bed shear and shields parameters would be the best areas to further investigate as defining an area of potential erosion/scour would be more helpful in these cases as erosion/scour is harder to rectify and more likely to cause issues in offshore wind farms than sediment deposition. This would enable an analysis of sediment deposition and intra array scale bed morphology evolution to be better predicted consequently bringing capital and monitoring costs of offshore wind farms down.

7.0 Conclusions

To conclude it was seen that the introduction of a Monopile into a marine environment at intra array level caused a variety of hydrodynamic and consequent inferred sediment effects. The reliability of obtained results was appraised, results are considered to be reliable due to the high level of post processing and careful data collection methods. The proposed Project I hypothesise (see section 2.0) has been confirmed to be correct as TKE decay at distance from the Monopile was seen to be affected by the angle of wave propagation, thus answering the main question behind this project.

Generic conclusions taken from the lab testing were that larger amounts of TKE can be found in the Monopile wake region when the angle of wave propagation aligns with that of the current direction and a larger amount of TKE can be found at free stream level when compared to bed level. It was also seen that the wake region rotated under wave propagation with maximum rotation achieved again when wave propagation angles and currents were more aligned. Less generic conclusions were also drawn from the lab experiments as the chosen experiment parameters

somewhat limited the transferability of results. Under wave and current conditions applied it was seen that TKE at bed level decayed to background levels in 8 diameters and at free stream level and 14 diameters along the downstream CL. No conclusive results were recorded within the bed shear part of the experiment however it was found that there were higher degrees of bed shear experienced without a Monopile present than at any point along the downstream CL of the Monopile.

The number of conclusions that were drawn from lab work is somewhat limited due to the limited data points and their positions, given further lab time more transects would have been employed. Bed shear stresses were only measured at distance from the Monopile along the downstream CL, this was unhelpful as it lay within an area of “still” water in the wake of the Monopile so did not provide any strong conclusions. Recommendations for further research based upon the above conclusions and their limitations are presented in the *Further proposed Research* Section 7.3.

In Appendix 1.0 both the predicted (Oct 2015) and achieved (Jan 2016) Gantt charts can be found showing a breakdown of tasks completed as part of project II. It can be seen that the main delay in the progress of project II is in the data analysis section, this is because of complications in construction of matlab scripts and the sheer amount of data requiring processing which was larger than predicted.

Project II has provided a great scope for additional in depth experimentation and learning around the subject of Monopile and wave/current interaction and has provided many conclusions and consequent opportunities for further research.

7.1. Links to previous research

In previous work Rogan (2015) concluded a number of matters from his experiment which was used as a foundation for the work undertaken in this project, such conclusions were compared to conclusions drawn in the light of recent work:

- The wave climate enhances dissipation of the turbulence generated by the Monopile.

It was shown that the presence of waves increases the level of TKE in the wake region of the Monopile and at free stream level more so than at bed level. In the presence of waves especially when they are more aligned with the current enhancement TKE decay can be seen at bed level. This is not seen at free stream level.

- It is shown that the modification of the turbulent wake is most significant when waves and currents are aligned, and less important when wave propagation is perpendicular to the current.

The wake region was seen to rotate and under all angles of wave propagation with angles similar to that of the current resulting in higher levels of TKE and consequent decay downstream.

- TKE decays to background levels at around 80 Monopile diameters

It was found that at bed level TKE along the downstream CL from the Monopile decayed to background level in 8 diameters not 80 as suggested by Rogan in this position with all wave propagation angles decaying to the same level. At free stream level it was observed it took 14 diameters with each angle of wave propagation decaying to its respective TKE level.

Magar et al. (2013) the other foundation document for this project came to the following conclusion that was consequently investigated in this project:

- Bed shear stresses generally satisfied a “law of the wall” equation.

This was found to be true to a distance from the bed of around 3.1cm along the downstream CL from the Monopile in all sampling positions observed.

Further to this both Magar et al. and Rogan spoke of further research to be undertaken in the areas of shear stresses, energy dissipation, scour and seabed impacts under varying hydrodynamic conditions and transport of suspended sediments in Monopile wake regions. Project II covers a few of these area in its scope and analysis however since no data was provided by Magar et al. or Rogan comparisons are not possible.

7.2. Real world application

The application of this work is intended to throw light on turbulence and consequent sediment effects in the wake region of offshore wind turbine Monopiles focusing on the combined current and wave interaction. At present there is a small body of research to provide accurate predictions of sediment and hydrodynamic effects post windfarm construction so there are associated high costs with monitoring and rectifying scour features. OFELIA (Offshore Foundations Environmental Impact Assessment) was an academic research partnership that aimed to quantify the implications of array construction (OFELIA, 2015). This project was undertaken in order to build on the foundation of existing works highlighted by OFELIA and research on Hydrodynamic and sediment effects resulting from the construction of offshore foundations with the eventual aim of future research being able to accurately predict sediment effects prior to construction. This will thereby reduce the initial capital and monitoring costs of offshore renewable wind power helping to make low carbon energy more accessible to the energy market. It is hoped in the long term this will help countries such as the UK achieve a carbonless energy mix and adhere to climate change targets such as COP21.

7.3 Further proposed research

From the work undertaken a number of further questions and areas requiring more research have made themselves known. Firstly all the experiments conducted have used only one wave and current condition, this had the advantage of being comparable to the chosen prototype site of Scroby Sands however this limited the transferability of conclusions and results. It is suggested a wider range of current and wave conditions are considered as this may yield more transferable results to Monopile and wave interaction problems. Additionally distance taken for TKE to decay to background levels e.g. decay of the wake region under a range of current conditions would be highly beneficial to draw conclusions from as there is limited amount of data about this available at the moment.

Secondly it is suggested a wider range of wave propagation angles are considered in the experiment as only three angles have been considered in this testing. This may be hard to model due to the inability to propagate currents at any other angle than across the tank in Plymouth coastal basin however the positioning of the Monopile may be adjusted in order to enable the consideration of wider angles of wave propagation.

Additionally the chosen location of data collection points is relatively sparse only using three transects and not fully utilising the traverse. Movement of the Monopile/traverse to further study the wake region (both locally and in the far field) from the Monopile and its evolution under varying waves and currents would present further opportunities to better understand the interaction between the structure and its environment. Wider radii and a denser net of data points would be advised in this case in order to better map vortices inferred/identified in this investigation.

Further analysis of particle fall velocities and vertical current velocities at prototype level within the wake region is another area that would benefit from detailed study. Further work in this area would help further explain sediment deposition features in the wake region, combining this study with that of bed shear stress a fuller picture of the downstream sediment environment can be constructed.

Lastly it is suggested more work in the area of bed shear is conducted within the locality of the Monopile and how it is affected by varying current and wave conditions. Specifically Bed Shear force calculated in this investigation used only X direction (downstream) flows to calculate Bed Shear, however a more robust calculation utilising both X and Y directions needs to be undertaken as this will give a more accurate representation of prototype processes. Further to this experimentation with different length sampling periods should be undertaken as using long sampling periods only takes into account the average current where as much sediment movement happens at maximum peaks in the current.

This should be a predominant area of further study as scour and sediment effects are a costly and dangerous side effect of offshore wind turbine construction. Prediction and better understanding of wave and current effects on the local sediment environment would yield many advantages to the industry. This research would reduce the need for costly environmental monitoring surveys and bringing the capital outlay and running/maintenance costs down by pre-empting and installing scour protection where needed. This reduction in the capital cost of offshore wind farms would be a driving force in the renewable energy industry helping to achieve carbon reductions as and renewable energy targets such as the 2020 EU targets (European Commission, 2014) and more recently the Paris COP21 targets.

Acknowledgements

Thanks are owed in my project to my supervisor Dave Simmonds for his guidance, Jon Miles for his input with data processing and Karin Needham for proof reading it!

References

CEFAS (2006) 'Scroby Sands Offshore Wind Farm – Coastal Processes Monitoring . Final Report for the Department of Trade and Industry Ecosystem Interactions', (July), pp. 1–51.

Crone, T. (no date) *The Basic Sediment Transport Equations Made Ridiculously Simple*, 2004. Available at: http://www.ocean.washington.edu/courses/oc410/reading/sedtrans_2004.pdf (Accessed: 4 March 2015).

Dight, M. (2013) 'Investigation into the change in hydrodynamic conditions and environmental impacts caused by the introduction of a wind turbine monopile to the marine environment', (September).

European Commission (2014) *The 2020 climate and energy package*. Available at: http://ec.europa.eu/clima/policies/package/index_en.htm.

Goring, D. G., Nikora, V. I. and Derek G, Goring; Vladimir I, N. (2002) *Despiking Acoustic Doppler Velocimeter Data*, *JOURNAL OF HYDRAULIC ENGINEERING*. Available at: http://imos-toolbox.googlecode.com/svn-history/r1283/wiki/documents/QC/CTD/goring_nikora02.pdf (Accessed: 10 November 2015).

Metoc plc (2000) 'An assessment of the environmental effects of Offshore Wind Farms', p. 67.

Miles, J. (2003) 'Matlab Denoising & Wave demodulation Scripts.'

OFELIA (2015) *OFELIA*. Available at: <http://www.interreg-ofelia.eu/> (Accessed: 15 February 2015).

Rogan, C., Miles, J., Simmonds, D. and Iglesias, G. (2015) 'The Hydrodynamics of Monopile Foundations - Experimental Measurements of Near Bed and Free Stream Turbulence', pp. 1–8. Available at: <http://www.crcnetbase.com/doi/abs/10.1201/b18973-115>.

Shearer, S. ; H. (no date) 'Fluid Mechanics: Stokes' Law and Viscosity.' Available at: [http://isites.harvard.edu/fs/docs/icb.topic1032465.files/Final Projects/Fluids Drag/stokes lab.pdf](http://isites.harvard.edu/fs/docs/icb.topic1032465.files/Final%20Projects/Fluids%20Drag/stokes%20lab.pdf) (Accessed: 17 March 2015).

Sumer, B.M.; Christiansen, N, Fredsøe, J. (1997) 'The Horseshoe Vortex and Vortex sheading around a vertical wall mounted cylinder exposed to waves', *Journal of Fluid Mechanics*, 332, pp. 41–70.

Stapelton, K; Huntley, D. (1995) 'Seabed Stress Determinations using the Inertial Dissipation Dethord and the Turbulent Kenetic Energy Methord', *Earth Surface Processes & Landforms*, 20(1), pp. 807–815.

Tumbler (no date) *Fluid Turbulence.Jpg*. Available at: https://41.media.tumblr.com/4262dc9237542247b4de06073cdb6eb0/tumblr_mvv5uuer1g1qckzoqp1_500.jpg (Accessed: 20 March 2015).

University of Illinois (no date) *Calculation of Bed Shear Stress Calculation of Bed Shear Stress, Geology Department*. Available at: [http://classes.geology.illinois.edu/11SprgClass/geo575/ALBDD Lecture 3 Calculation of Shear Stress.pdf](http://classes.geology.illinois.edu/11SprgClass/geo575/ALBDD%20Lecture%203%20Calculation%20of%20Shear%20Stress.pdf) (Accessed: 10 March 2015).

USGS (2008) *Simulation of Flow, Sediment Transport, and Sediment Mobility of the*

Lower Coeur d'Alene River, Idaho, Scientific Investigations Report. Available at: <http://pubs.usgs.gov/sir/2008/5093/table7.html> (Accessed: 10 March 2015).

Vanhellemont, Q. and Ruddick, K. (2014) 'Turbid wakes associated with offshore wind turbines observed with Landsat 8', *Remote Sensing of Environment*. The Authors, 145, pp. 105–115. doi: 10.1016/j.rse.2014.01.009.

Vassalos, D. (1999) 'Physical modelling and similitude of marine structures', 26, pp. 111–123. doi: 10.1016/S0029-8018(97)10004-X.

Appendices for this work can be retrieved within the Supplementary Files folder which is located in the Reading Tools menu adjacent to this PDF window.